Jurnal Teknologi

Full Paper

INVESTIGATION OF GRAPHENE CHANNEL INTERACTION WITH YEAST CELL FOR CELL COUNTING APPLICATION

Fatin Norshafini Zainol, Muhammad Syazwan Dollah, Mohd Ridzuan Ahmad, Shaharin Fadzli Abd Rahman*

Faculty of Electrical Engineering, Universiti Teknologi Malaysia, 81310 UTM Johor Bahru, Johor, Malaysia

Article history
Received
30 October 2015
Received in revised form
8 March 2016
Accepted
28 March 2016

*Corresponding author
shaharinfadzli@utm.my

Graphical abstract

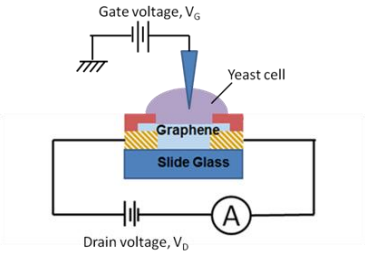

Abstract

Graphene superior and unique properties make it a suitable material for biosensor. In this work, graphene interaction with yeast cell is investigated for development of graphene-based cell counter. The fabricated graphene channel was characterized by means of two-terminal and solution-gated three-terminal measurement setup. The correlation between graphene channel resistance and cell concentration was confirmed. The yeast cell was found to give n-type doping which modulate the conductivity of graphene channel.

Keywords: Graphene, cell counting, yeast cell

Abstrak

Ciri grafin yang unggul dan unik menjadikan ia bahan yang sesuai untuk biosensor. Pada kerja ini, interaksi antara saluran grafin dan sel yis disiasat untuk pembangunan pengira sel dari grafin. Saluran grafin yang telah difabrikasi telah dicirikan dengan cara pengukuran dua-terminal dan cecair-get tiga-terminal. Korelasi antara rintangan saluran grafin dan kepekatan cell telah disahkan. Yis sel didapati memberikan kesan pendopan jenis-n yang mengubah kondiktiviti saluran grafin.

Kata kunci: Grafin, pengiraan sel, sel yis

1.0 INTRODUCTION

Graphene, a single-atomic-layer of carbon atoms bonded together in hexagons pattern, is a unique nanomaterial, which has attracted enormous attention since its discovery in 2004 [1]. Due to its high sensitivity to various adsorbates, large surface-to-volume ratio, unique optical properties and excellent electrical conductivity, graphene has been rapidly investigated for the development of various types of sensors such as humidity sensor and pH sensor [2-4]. Its sensor application can be extended to biomedical field [5-7]. The large surface area of graphene enhances the surface contact with the desired biomolecules that leads to the high sensitivity. For example, a multi-layer graphene attached with antibody was shown to have better sensitivity to cancer risk biomarker compared to other method [5]. In another graphene biosensor, metabolic activity of cell could be monitored based on the pH level [7]. The high sensitivity of graphene biosensor can also be associated to good electron conduction between the biomolecules and graphene, due to its zero bandgap. Furthermore, graphene's high optical transparency also allows real-time monitoring and characterization of the moving biomolecules.

In recent years, several efforts have been made to utilize graphene for biological cell analysis [6, 7]. The ultimate motivation is to enable cell analysis at single-cell level, which will contribute towards improved diagnosis, prognosis, and treatment of critical diseases such as cancer. P. K. Ang *et al*. have

demonstrated that malaria-infected red bloods cell could be distinguished from healthy cells by incorporating solution-gated graphene field-effect transistor with microfluidic channel [6]. Besides of analysis at single cell level, analysis of a cell group or population is also significance. Cell counting is a common and simple technique to determine the health and to reveal information about the progress of infectious diseases. The cell counting can be performed in various techniques such as manual calculation using hemocytometer, coulter counter, flow cytometry and image processing [8-11]. Manual calculation using hemocytometer is a very simple and low-cost approach [8]. However, the reading is prone to error caused by the examiner. On the other hand, coulter counter and flow cytometry are more reliable tools [9]. The counting may take some time as the cell is counted one by one. By utilizing graphene, accurate and fast counting could be realized. Owing to graphene's high sensitivity, the signal from cell population could be translated to the number of cell.

Nevertheless, up to date, number of specific work on cell-based graphene biosensor is relatively low. More works is required in order to provide better understanding especially regarding the interaction between cell and graphene channel. In this work, we investigate the interaction between cell solution and electrical properties of graphene channel. Note that this work focuses on analyzing cell population (i.e. cell solution) rather than at single-cell level. The finding from this work is expected to contribute to the development of graphene-based cell counter. For this experiment, yeast cell is used to represent human cell as it can be easily obtained and possesses strong similarities to human cell. The correlation between numbers of cell with graphene channel resistance is investigated and discussed.

2.0 EXPERIMENTAL

2.1 Device Fabrication

Figure 1 shows the process flow of device fabrication. The fabrication process involves three stages, which are electrode formation, graphene transfer and deposition of encapsulation layer. A transparent glass slide was used as the substrate. This is to allow direct observation of yeast cell solution under microscope.

Fabrication was started with formation of two-terminal gold electrode. The electrode was formed by photolithography and plasma sputtering process. The gap between the electrodes was 1.5 mm. Then, single-layer graphene grown on copper foil, which purchased from Graphenea Inc. (Spain) was transferred onto the substrate connecting the two gold electrodes. The purchased graphene film is claimed to have optical transparency above 97% and film continuity above 98%. Graphene transfer was done by etching out the underlying copper foil by using ferric chloride solution (1 M $FeCl_3$). Prior to the etching, graphene was coated by polymethyl methacrylate (PMMA). The PMMA layer functions as mechanical support which holds together the thin graphene film during the etching and transfer process. After the etching, PMMA-coated graphene sheet was transferred onto desired location. PMMA was removed by acetone after the completion of transfer process.

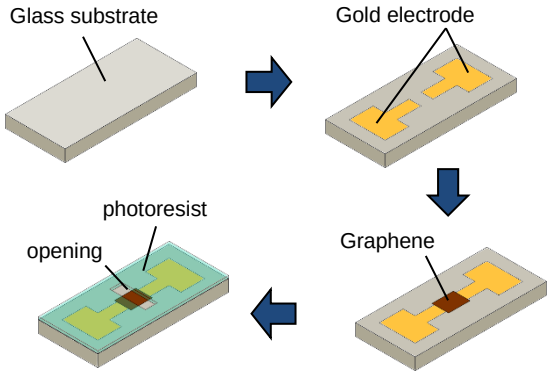

Figure 1 Device fabrication process flow

The device fabrication was completed by depositing encapsulation layer using printed-circuit-board photoresist. The function of encapsulation layer is to protect areas other than graphene layer from being contacted with yeast cell solution. The photoresist was coated onto substrate by spin coating and baked on hotplate. An opening area on graphene layer was defined by exposing the intended area with UV light and immersing into the developer solution. This uncovered area is the opening area where yeast cell solution is dropped. The length of opening layer is 1 mm. The formation of the opening area was confirmed with bare eye and microscope. The sample was further baked on hotplate at 120 °C for 30 minutes. This is to improve chemical resistance of the coated photoresist layer. In order to confirm the presence of graphene after the aforementioned process, electrical continuity test was performed across the electrodes. The finite resistance indicates that the graphene is still attached onto the glass substrate and makes connection between the electrodes.

Figure 2 shows a camera image and cross-sectional schematic of the fabricated device. Dashed lines highlight the opening area between the electrode gap. Green colored area is the area coated with photoresist. Dashed line outlines the opening area.

2.2 Electrical Characterization at Different Cell Solution

Prior to current-voltage (I-V) measurement, yeast cell solution was prepared. The yeast cell solution was

prepared using commercial instant yeast (Mauri-pan instant yeast). One tablespoon (14.8 ml) of instant yeast was added into warm sugar solution (44 - 49 °C). The sugar supplies energy to the yeast for its living and growth. The mixture was left for 24 hours. The yeast cell concentration was varied by diluting the mixture with deionized water. Methylene blue solution (0.1% m/v) was added to each diluted cell solution in ratio of 1:1 to check the viability of the yeast cell. The prepared solutions was then injected into opening area of the graphene channel and observed under the microscope. 10 images of yeast cell were taken randomly at 10 different locations bounded at the opening area. Number of cell in every image was manually counted and averaged. Number of cell per unit area was calculated by dividing average cell number with area of the image (0.082 mm^2).

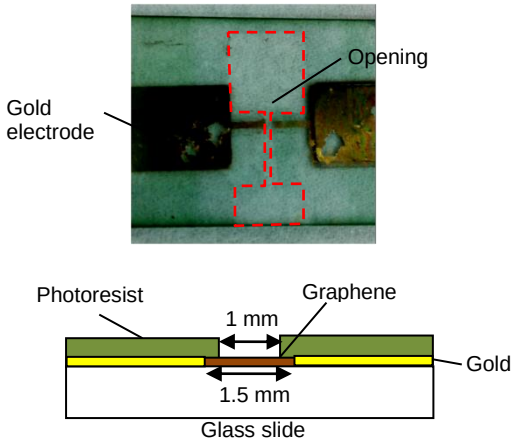

Figure 2 Camera image and cross-sectional schematic of the fabricated device

Two I-V measurement configurations were applied in order to investigate the interaction between cell and graphene channel. The configurations were two-terminal and solution-gated three-terminal setup. Figure 3 shows the measurement setup for the two configurations. Graphene channel resistance was measured at various cell concentrations. For solution-gated setup, a tungsten needle was used as the gate electrode. The gate voltage was varied to obtain transfer characteristic of solution-gated graphene transistor. All the I-V measurements were implemented using source measure unit (Keithley model 2400). All the yeast solutions were assumed to have almost similar temperature, thus the effect of solution temperature could be ignored.

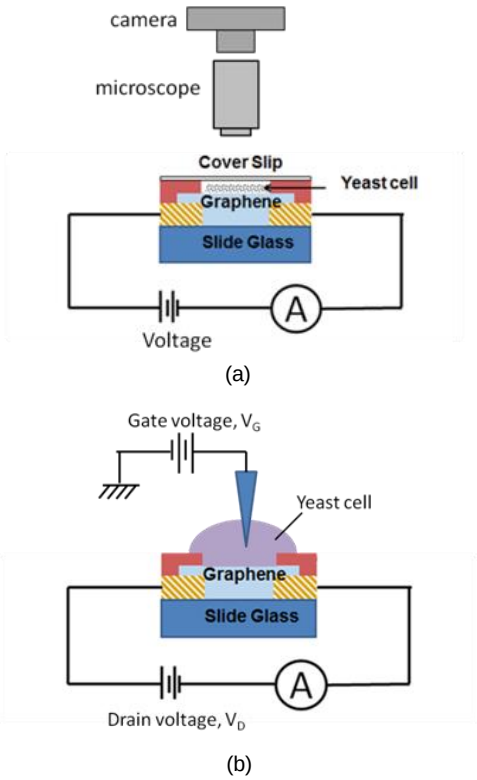

Figure 3 Measurement setup for (a) two-terminal and (b) solution-gated three-terminal configuration

3.0 RESULTS AND DISCUSSION

3.1 Two-terminal Measurement

Figure 4 shows I-V characteristic of graphene channel when yeast cell solutions with various concentrations were dropped onto the opening area. Measurement using the methylene blue solution (i.e. absence of yeast cell) was also done and plotted in Figure 4. In case of when using methylene blue solution, a linear I-V characteristic was observed. The graphene could be represented by a channel with a finite resistance. However, when yeast cell solution was added, the experimental result showed nonlinear curves. The nonlinear curve could be as a result of the change in electrostatic potential of graphene channel due to doping effect by yeast cell solution. Another interesting point from the result was the observation of the non-negligible short-circuit current. The short-circuit current is the measured current at zero bias. Without yeast cell (i.e. methelyne blue solution), the short-circuit current is negligible. The current value was shown to be dependent to the cell concentration. The origin of the short-circuit current is still unclear. It can be due to leakage current through encapsulation layer, or due to the carrier movement induced by potential created by the yeast cell solution.

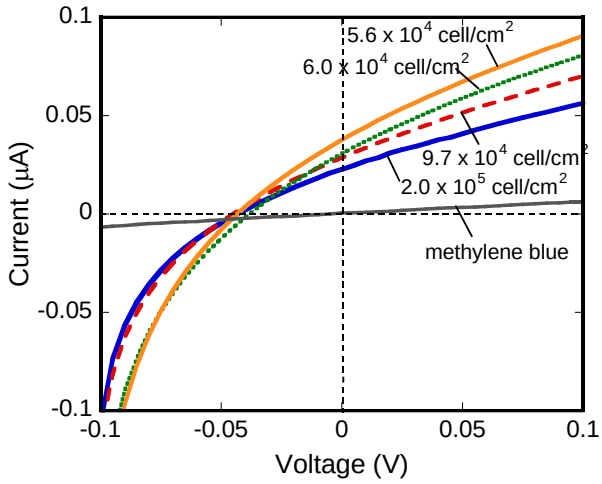

Figure 4 I-V characteristics at various cell concentration

From the measured nonlinear I-V curve, average dynamic resistance was calculated. The dynamic resistance was calculated by considering current change in voltage range of 0 to 0.1 V. Relationship between cell concentration and the calculated average resistance is shown in Figure 5. Channel resistance was found to increase when cell concentration increases. The sensitivity of the fabricated sensor was calculated to be 12 Ω/(cell.cm^{-2}) at low cell concentration. At higher cell concentration, the channel resistance value saturated. The sensitivity at this region was 0.18 Ω/(cell.cm^{-2}). The reason of the observed trend is discussed at section 3.3.

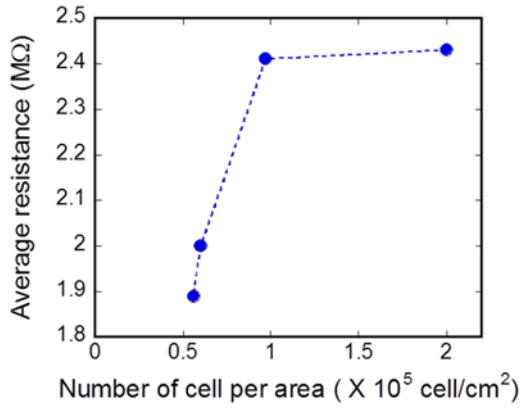

Figure 5 Average AC resistance versus number of cell per area

3.2 Solution-gated three-terminal Measurement

The Interaction between cell and graphene can be further analyzed from the result of three-terminal measurement. In solution-gated three-terminal measurement setup, an operation of graphene transistor should be observed. Figure 6 shows an output characteristic of the solution-gated graphene transistor at cell concentration of 1.92 x 10^6 cell/cm^2. Current saturation was observed in particular at gate voltage, V_G of 0.2 and 0.4 V. As V_G decreased from 0.6 to 0 V, the drain current decreased. This was the condition where graphene behaved as an n-type material. When V_G was further decreased below 0 V, the drain current increased. At this operating region (V_G < 0 V), graphene behaved as p-type channel. The observation of n- and p-type behaviour was an evidence of ambipolar characteristic of graphene channel.

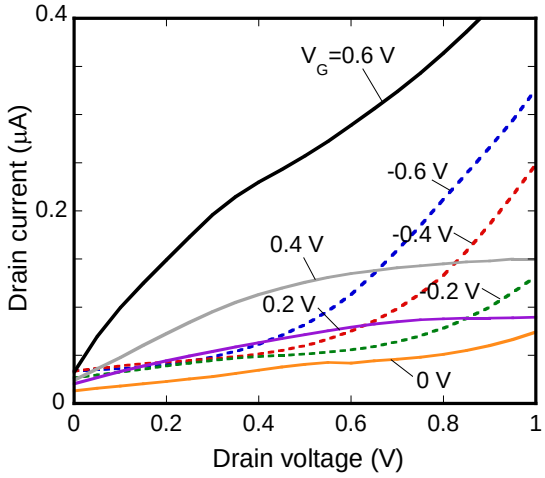

Figure 6 Output characteristic of solution-gated graphene channel at cell concentration of 1.9 x 10^6 cell/cm^2

The ambipolar characteristic of solution-gated graphene channel can be clearly observed by plotting transfer characteristic of the device. Values of the drain current for different gate voltage were extracted at drain voltage of 1 V. Figure 7 shows the plotted transfer characteristic at different cell concentration. A V-shaped transfer curve reflects the two types of conductions (i.e. electron and hole). At low cell concentration, a slight positive shift of the transfer characteristics was observed. Conduction of n-type channel was found to decrease at low cell concentration.

3.3 Discussion

Positive shift of the transfer characteristics (i.e. positive Dirac point shift) as well as suppression of electron conduction in Figure 7 are signs of p-type doping effect [12]. D. B. Farmer *et al*. have related the suppression of electron conduction to misalignment of channel and electrode neutrality points [12]. It could be concluded that solution with lower cell concentration gives higher p-type doping effect.

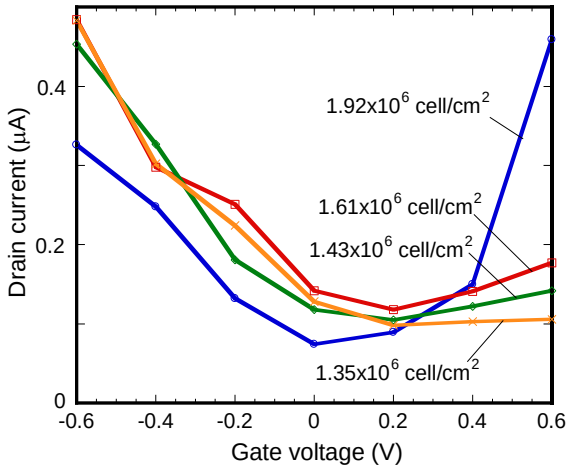

Figure 7 Transfer characteristic of solution-gated graphene channel at different cell concentration

The p-type doping effect is most likely come from deionized water in yeast solution. Water is well-known as p-type dopant of graphene channel [13]. The doping of graphene channel is achieved by surface charge transfer between graphene and water due to chemical potential difference [14]. At lower cell concentration p-type doping by water becomes dominant. At higher cell concentration, the p-type doping of water is reduced. We claimed that the p-type doping is balanced by n-type doping from yeast cell.

Our speculated mechanism explained the obtained result from two-terminal measurement shown in Figure 5. The fabricated device can be considered to be p-type doped by water that used throughout the device fabrication [13]. When cell concentration increased, the n-type doping effect increased. Thus, overall hole concentration decreased and subsequently increase the channel resistance. Channel resistance increases until a point where graphene switches to n-type channel. Note that near the transition point, the change of resistance is relatively small. This explains why resistance value seemed to be saturated at high yeast cell concentration.

4.0 CONCLUSION

Graphene channel was fabricated and its interaction with yeast cell solution was analyzed for the development of graphene-based cell counter. Yeast cell was used to represent human cell. Electrical characterization was performed using two configurations; two-terminal and solution-gated three-terminal setups. The obtained results indicated that yeast cell influences the resistance of graphene channel. The yeast cell is speculated to function as n-type dopant to the graphene channel. Further thorough investigation is highly required to verify the speculated mechanism. Nevertheless, this work exhibited the promising potential of graphene in particular as a cell counter.

Acknowledgement

This work is partly supported by university grants (Potential Academic Staff Grant and Research Group Flagship) from Universiti Teknologi Malaysia.

References

[1] Novoselov, K. S., A. K. Geim, S. V. Morozov, D. Jiang, Y. Zhang, S. V. Dubonos, I. V. Grigorieva, and A. A. Firsov. 2004. Electric Field Effect in Atomically Thin Carbon Films. *Science*. 306: 666-669.

[2] Meng-Chu, C., H. Cheng-Liang, and H. Ting-Jen. 2014. Fabrication of Humidity Sensor Based on Bilayer Graphene. *IEEE Electron Device Letters*. 35: 590-592.

[3] Lei, N., P. Li, W. Xue, and J. Xu. 2011. Simple Graphene Chemiresistors as pH Sensors: Fabrication and Characterization. *Measurement Science and Technology*. 22: 107002.

[4] Mailly-Giacchetti, B., A. Hsu, H. Wang, V. Vinciguerra, F. Pappalardo, L. Occhipinti, E. Guidetti, S. Coffa, J. Kong, and T. Palacios. 2013. pH Sensing Properties of Graphene Solution-Gated Field-Effect Transistors. *Journal of Applied Physics*. 114: 084505.

[5] Tehrani, Z., G. Burwell, M. A. M. Azmi, A. Castaing, R. Rickman, J. Almarashi, P. Dunstan, A. M. Beigi, S. H. Doak, and O. J. Guy. 2014. Generic Epitaxial Graphene Biosensors for Ultrasensitive Detection of Cancer Risk Biomarker. *2D Materials.* 1: 025004.

[6] Ang, P. K., A. Li, M. Jaiswal, Y. Wang, H. W. Hou, J. T. L. Thong, C. T. Lim, and K. P. Loh. 2011. Flow Sensing of Single Cell by Graphene Transistor in a Microfluidic Channel. *Nano Letters*. 11: 5240-5246.

[7] Paulus, G. L. C., J. T. Nelson, K. Y. Lee, Q. H. Wang, N. F. Reuel, B. R. Grassbaugh, S. Kruss, M. P. Landry, J. W. Kang, E. Vander Ende, J. Zhang, B. Mu, R. R. Dasari, C. F. Opel, K. D. Wittrup, and M. S. Strano. 2014. A Graphene-Based Physiometer Array for the Analysis of Single Biological Cells. *Scientific Reports*. 4: 6865.

[8] Absher, M. 1973. *Tissue Culture: Methods and Applications*. Academic Press.

[9] Graham, M. D. 2003. The Coulter Principle: Foundation of an Industry. *Journal of the Association for Laboratory Automation*. 8: 72-81.

[10] Boyd, A. R., T. S. Gunasekera, P. V. Attfield, K. Simic, S. F. Vincent, and D. A. Veal. 2003. A Flow-Cytometric Method for Determination of Yeast Viability and Cell Number in a Brewery. *FEMS Yeast Research*. 3: 11–16.

[11] Hong, D., G. Lee, N. C. Jung, and M. Jeon. 2013. Fast Automated Yeast Cell Counting Algorithm using Bright-Field and Fluorescence Microscopic Images. *Biological Procedures Online*. 15: 13.

[12] Farmer, D. B., R. Golizadeh-Mojarad, V. Perebeinos, Y.-M. Lin, G. S. Tulevski, J. C. Tsang, and P. Avouris. 2009. Chemical Doping and Electron−Hole Conduction Asymmetry in Graphene Devices. *Nano Letters*. 9: 388-392.

[13] Ni, Z. H., H. M. Wang, Z. Q. Luo, Y. Y. Wang, T. Yu, Y. H. Wu, and Z. X. Shen. 2010. The Effect of Vacuum Annealing on Graphene. *Journal of Raman Spectroscopy*. 41: 479-483.

[14] Liu, H., Y. Liu, and D. Zhu. 2011. Chemical Doping of Graphene. *Journal of Materials Chemistry*. 21: 3335-3345.